

Dynamic Mechanical Moduli of Residual Softwood-Filled Polystyrene

Mahmoud Abdel-Goad

Department of Petroleum and Chemical Engineering, College of Engineering, Sultan Qaboos University, P.O. Box 33, PC 123, Al-Khoud, Muscat, Sultanate of Oman

Received 6 September 2007; Accepted 10 March 2008

خصائص الميكانيكا الديناميكية للبولي استيرين المحشو بقايا الخشب اللينة

محمود عبد الجواد

الغلاصة: تمت إضافة بقايا نشارة الخشب إلى البولي استيرين ذي الوزن الجزيئي العالي (٢٨٠٠٠ جم/مول). تم تحضير البولي استيرين المخلط بطريقة خلط المصهور. الخصائص الريولوجية تم تحديدها بواسطة جهاز الريوموميتر عد درجات حرارة ما بين ١٤٠ إلى ٢٤٠ درجة مئوية و تردد ما بين ١ إلى ١٠٠ لفة/ثانية. ومن البحث تبين ان الخصائص الريولوجية قد تحسنت كثيرا باضافة هذه المخلفات الخشبية إلى البولي استيرين مما يمكن استخدامها على نطاق اوسع كماده بلاستيكية.

المفردات المفتاحية: نشارة الخشب اللين ، الخليط ، التحليل الميكانيكي الحركي ، الزوجة .

Abstract: Residual softwood sawdust (RSS) was added to polystyrene (PS) that has molecular weight 280000 g/mol. The PS composite was prepared by melt mixing technique. The dynamic mechanical tests are carried out using ARES-rheometer (Rheometric Scientific, USA) in the dynamic mode and parallel plate geometry with diameter 25 mm. The measurements were performed at temperatures ranging from 140 to 240°C and frequencies varied from 0.1 to 100 rad/s at strain 1% and gap setting 2 mm. The dynamic mechanical properties in terms of complex modulus, G^* , torque, compliance moduli, loss tangent and complex viscosity has been studied for fiber-filled PS composite. The viscoelastic properties of the filled and unfilled systems have been compared. These properties are found to be improved by the addition of RSS. The dynamic mechanical moduli and viscosity were found to rise with fiber loading.

Keywords: Residual softwood sawdust, Composite, Dynamic mechanical analyzer, Shear creep, Stress relaxation, Melt viscosity

1. Introduction

Filled polymer composites are attracting ever growing interest. Therefore, a lot of research work has been carried out on reinforced polymers composites (Fang, Z. and Hu, Q., 1999; Mitsubishi, K., 1997; Lee, K.M. and Han, C.D., 2003; Hu, X., et al. 2003; MCGinness, G.B. and Bradaigh, C.M.O., 1997; Kim, J.I., Ryu, S.H. and Chang, Y.W., 2000; Tavman, J.H., 1996; Solomon, M.J., et al. 2001; Marchant, D. and Jayaraman, K., 2002; Ray, S.S., Maiti, P., Okamoto, M., Yamada, K. and Ueda, K., 2002; Zhang, Q. and Archer, L.A., 2002; Wang, Z., Wu, Q., Dong, J., Hu, Y. and Qi, Z., 2002; Roy, D., Bhowmick, A.K. and De, S.K., 1993; Nam, J.D. and Sefferis, J.C., 1999). Fiber-reinforced plastic composites began with cellulose fiber in phenolics in 1908, later extending to urea and melamine, and reaching commodity status in the 1940s with glass

fiber in unsaturated polyesters (Mohanty, A.K. Misra, M. and Hinrichsen, G., 2000). Nowadays mineral fillers and fibers are extensively used in the plastics industry to achieve desired properties or to reduce the price of the finished article (Angles, M.N., Salvado, J. and Dufresne, A., 1999). The importance of fiber-filled composites arises largely from the fact that such materials can have unusually high strength and stiffness for a given weight of material. In addition, there is an increasing interest in environmental concerns. It is incorporated to maximize the use of renewable resources and also to minimize the wastes. So the valorization of a lignocellulosic residual material and its use as a lightweight and economical source of reinforcement in thermoplastic composites has received substantial attention (Angles, M.N., Salvado, J. and Dufresne, A., 1999). Lignocellulosic materials are the most abundant renewable biomaterial of photosynthesis on earth (Mohanty, A.K. Misra, M. and Hinrichsen, G., 2000). Compared to inorganic fillers, the main advantages of lignocellulosics are their renewable nature, wide variety of

fillers available throughout the world, nonfood agricultural-based economy, low energy consumption, cost and density, high specific strength and modulus, high sound attenuation of lignocellulosic-based composites, comparatively easy processability due to their nonabrasive nature, which allows high filling levels, resulting in significant cost savings, and relatively reactive surface, which can be used for grafting specific groups. Moreover, the recycling by combustion of lignocellulosic-filled composites is easier compared to inorganic fillers systems. Therefore, the possibility of using lignocellulosic fillers in the plastic industry has received considerable interest and the study of cellulosic materials reinforced polymer composites that contain cellulosic materials has been recognized as an important area of research for over a decade (Bledzki, A.K., Reihmane, S. and Gassan, J., 1996; George, J., Bhagawan, S.S., Prabhakaran, N. and Thomas, S., 1995; Lowys, M.P., Desbrieres, J. and Rinaudo, M., 2000; Felix, J.M. and Gatenholm, P., 1991; Swerin, A., 1998; Gatenholm, P., Bertilsson, H. and Mathaiasson, A., 1993).

Environmental concerns generated by plastic materials are generating an increasing interest toward the development of ecological products. The use of disposable plastics increases the undegradable waste portion, for this reason, it is necessary to develop more recyclable and/or biodegradable plastics to reduce the amount of landfill. Where that method of land-filling will prevent the plant roots to grow and as a result the agriculture will negatively be affected. In addition plastics waste has considerable volume since the weight of it in the waste stream is only 8 percent, but it takes up nearly 20 percent of the volume in landfills.

The composites of natural fibers and non-biodegradable synthetic polymers may offer a new class of materials, but are not completely biodegradable. The designing materials compatible with the environment becomes the target from the government regulations and growing environmental awareness throughout the world.

Dynamic mechanical tests give more information about a composite material than other tests. The tests, over a wide range of temperatures and frequencies, are especially sensitive to all kinds of relaxation process of matrix resin and also to the morphology of the composites. DMA is a sensitive and versatile thermal analysis technique, which measures the modulus (stiffness) and damping properties (energy dissipation) of materials as the material are deformed under periodic stress (Saha, A.K., Das, S., Bhatta, D. and Mitra, B.C., 1999). Since polymer melt flow behavior is strongly affected by the nature of the filler type, including its morphology, surface chemistry and concentration, rheological studies can also assist in the development of formulations designed to facilitate industrial processability.

The motivation of this work is to prepare biodegradable polystyrene composite by adding waste agricultural residues (residual softwood sawdust (RSS)) to commercial polystyrene and analysis this composite mechanically compared to the original material of neat polystyrene.

2. Experimental Part

2.1 Materials and Preparation

In this study PS composite was prepared by adding commercial PS to residual softwood sawdust. The PS used has high molecular weight of 280000 g/mol (280K). Saw dust used in this study is waste agricultural residues (residual softwood sawdust (RSS)) Which was provided from Egypt. The residual softwood sawdust was prepared by drying and shredding in a particle size of about 1mm. 7 wt% fibers were added to the PS. The size of the fiber is expected to be lower than millimeter scale after mixing with molten PS. Composite samples were prepared by dry mixing homogeneously the fiber with the polymer followed by melt mixing at about 300°C for 2 hours because the glass transition temperature of neat polystyrene is 100°C, fillers shift the glass transition temperatures that means 300°C was chosen as the lowest temperature needed for 2 hours to incorporate the fiber into polystyrene with molecular weight 280000 g/mol. The samples were prepared under that condition (300°C for 2 hours) to ensure getting homogeneous distribution of the fibers throughout the polymer sample. Molten-sate sample (at 300°C) was molded at 5 bars for 30 minutes.

The samples were shaped in the disc form with diameter around 25 mm and thickness about 2 mm. The samples of neat PS were moulded also with the same dimensions of 25 mm diameter and 2 mm thickness at about 250°C under 5 bars for about 30 minutes.

2.2 Instrument and Measurements

The melt rheological properties of the material were determined using ARES-rheometer (Rheometric Scientifics, USA). The ARES instrument is a modular and extendable rheometer works under nitrogen atmosphere in a wide range of temperatures and frequencies. During testing at or above ambient temperature, gaseous nitrogen is used. The sample to be tested is positioned between two plates in the test station. Upper plate is connected to the transducer and lower plated is connected to motor. Before placing the sample, the normal force of the system should be kept around zero. The sample is positioned on the lower plate followed by lowering the stage until the sample just contacts the upper plate completely. The actual gap size is read electronically and this allows absolute moduli to be determined. In this work the measurements were performed in the dynamic mode and 25 mm parallel plates geometry with gap settings about 2 millimeters. The soak time at the measuring temperature was 4 minutes. That soaking time is required to transfer the heat homogeneously throughout the sandwiched samples between the plates and stabilizing the temperature before starting the measurement. The strain amplitude was kept to be 1% in the whole frequency range to ensure linearity and 8 points per frequency-decade were obtained. The samples were measured in a range of temperature from 140 to 240°C with interval temperature 10°C as a function of frequency.

The frequency ω , varied from 10^{-1} and 10^2 rad/s. Horizontal and vertical shift factors were obtained from a two dimensional shifting.

3. Results and Discussion

The log-log curves of the data measured at different temperatures were superposed into master curve at a reference temperature, T_0 , by shifting in the horizontal and vertical directions as shown in Fig. 1. In this Figure the shear complex modulus (G^*) is plotted for unshifted and shifted data as a function of frequency. G^* decreases with increase the temperature as seen in the case of unshifted data. The experimental data were shifted into a single curve (master curve) by using of the time-temperature superposition principle which described by (Ferry, J.D., 1980) as:

$$\log a_T = \log \frac{\tau(T)}{\tau(T_0)} = \frac{-c_1(T-T_0)}{c_2 + (T-T_0)}$$

Where a_T is the empirically derived shift factor and constants C_1 and C_2 are material specific and their values are listed in Table 1. T_0 is chosen in this study to be 160°C . Table 1 shows variation in the shifting accuracy from sample to sample. That indicates the difficulties in shifting such materials (composites) using WLF principle unlike linear homopolymeric materials.

The a_T shifts the data obtained at different temperatures along the log frequency, ω axis as shown in Fig.1 and in vertical direction is given purely by b_T ($b_T = \rho_T / \rho_T T_0$ Pearson, D., Fetters, L. and Grassley, W., 1994). Where ρ is the material density and the shift factors for these samples are plotted with respect to temperature in Fig. 2. a_T decreases by increasing the temperatures up to a certain limit then becomes somewhat independent on the temperature. b_T is nearly independent on the temperatures up to around 200°C then decreases by increasing the temperature as shown in Fig. 2.

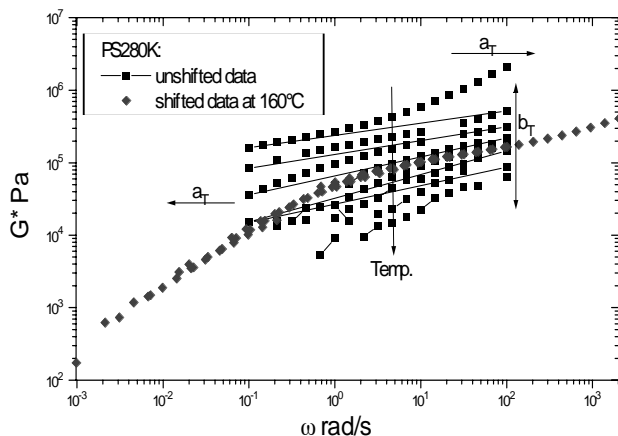


Figure 1. The complex modulus of PS280K as a function of frequency

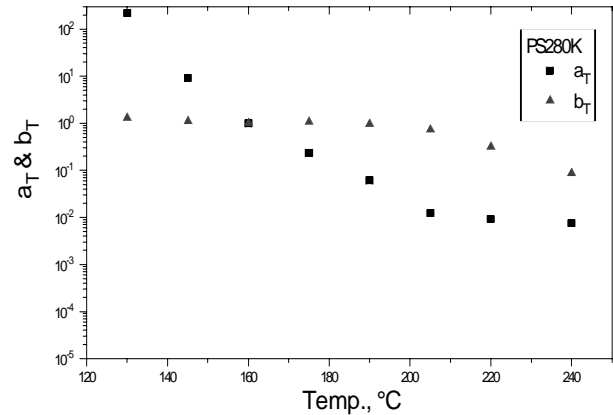


Figure 2. a_T and b_T vs. temperature

Table 1. WLF constants of PS and PS composites at $T_0 = 160^\circ\text{C}$

Polymer	C_1	C_2	r^2
PS280K	6.16	94.92	0.98
PS280K/7%CF	3.46	67.77	0.72
PS280K/9%CF	6.85	172.15	0.88

The master curves of the shear complex modulus, G^* for the fiber-filled and unfilled PS at 160°C is logarithmically plotted against the frequency (angular) in Fig. 3. This quantity of G^* can be resolved into real (G') and imaginary (G'') components such that $G^* = G' + i G''$ (Heinrich, G. and Kluppel, M., 2002). Where G' is the ability of the material to store energy in the cycle of the deformation, for that it is called storage modulus and G'' is defined as the ability of the material to dissipate the energy per cycle of the deformation and it is called loss energy. The dynamic spectrum of shear storage modulus (G') and shear loss modulus (G'') with respect to frequency contains information regarding the manner in which a sample responds to small magnitude deformation applied over varying temperatures and time scale. The master curve of G^* displays three distinct regions of behavior and that is typically for flexible-chain monodisperse homopolymer as the glass transition, rubbery plateau, and terminal zones when going from high frequency to low frequency. The glass transition zone is the regime between the glass and rubber-like zones at which the deformation frequency is high compared to the average relaxation time of the polymer chain. Since some molecular chain segments can not move while some are free to move. If the stress is initially applied, the segment will move in such a manner as to reduce the stress on it. After moving, the segment has less stored energy because of the reduction in stress, so the excess energy was dissipated as heat and the observed modulus is high as shown in Fig. 3. As the frequency of deformation decreases, G^* decreases until the intermediate at which the rubbery plateau is observed. This rubbery plateau region is independent on the frequency (the flatness of $G^*(\omega)$) over several decades of frequency as seen in Fig. 3. It reflects the rubber-like

properties of the polymer and indicating that polymer chains have sufficient time to relax locally but at adequately high molecular weights are entangled and exhibit behavior consistent with rubbery network (network like structure reflects in rubbery regime). Figure 3 shows that G^* modulus for the filled PS with 7% RSS is higher than this of neat PS. Numerically at around 50 radians/s the value of G^* increased from 0.15 to 0.23 MPa by the incorporation of 7% filler.

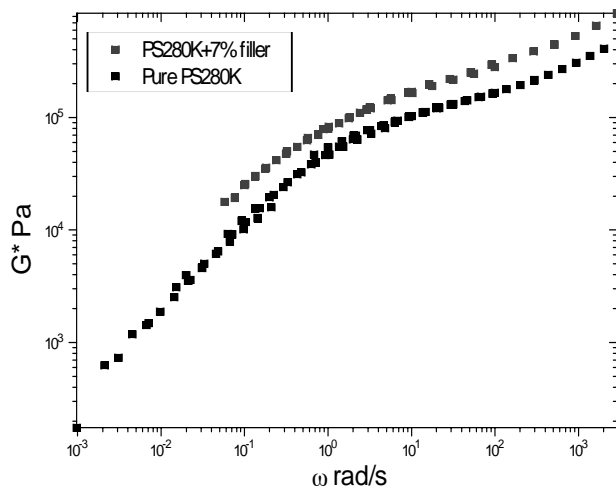


Figure 3. Master curve of G^* for filled and unfilled PS280K vs ω at $T_0 = 160^\circ\text{C}$

Generally speaking, the incorporation of fibers as fillers into polymeric material matrix results in high specific strength and modulus for polymer composites based on those fillers. Moreover, these fillers have easy processability due to their nonabrasive nature, which allows high filling levels therefore resulting in enhancing the cross links density hence the physical network structure. Their nonabrasive nature also leads to relatively reactive surface, which can be used for grafting specific groups of polymers, accordingly, the density of chemical cross links increases.

As shown in the results the complex modulus increases by introducing of filler in polystyrene. The main reason, which can be summarized from the explanation above, is because of the formation of the physical polymer-fiber network, which leads to increase the strength of the PS composite. Here, the contribution of the chemical cross links can not be completely ignored since it can be formed even as non-significant contribution compared to the physical network like structure.

Similar results are shown in Figs. 4 and 5 for the shear compliance (the storage and loss compliance). The storage, $J'(\omega)$ and loss, $J''(\omega)$ compliance are plotted with logarithmic scale in Figs. 4-5. $J'(\omega)$ is a measure of the energy stored and recovered per deformation cycle, therefore it is called the storage compliance. $J''(\omega)$ is a measure of the energy dissipated as heat per cycle of the sinusoidal deformation, for that is called the loss compliance. The plot of $J'(\omega)$ has roughly the appearance of mirror image

of G^* plot reflected in the frequency axis. Figures 4 and 5 represent three distinct regions of behavior as explained above for G^* modulus. However, the intermediate regime (plateau regime in Fig. 4 and rubbery in Fig. 5) can not be clearly seen in these figures for insufficient high molecular weights of polystyrene. Additionally, the effect of thermal degradation can not be ignored that may be occurred under the preparation conditions of PS composites (at 300°C for 2 hours).

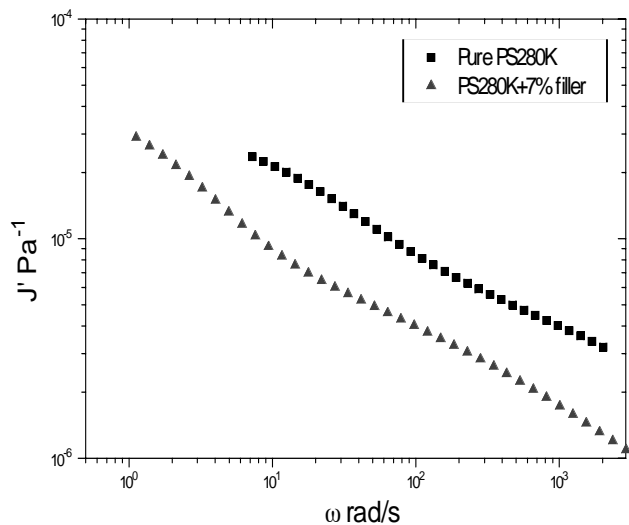


Figure 4. Master curve of J' for filled and unfilled PS280K vs ω at $T_0 = 160^\circ\text{C}$

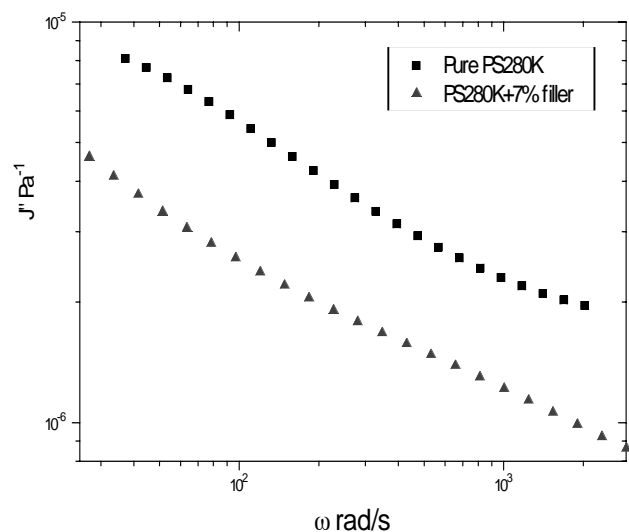


Figure 5. Master curve of J'' for filled and unfilled PS280K vs ω at $T_0 = 160^\circ\text{C}$

The same effect of the addition of RSS is found in the shear compliance where the decrease in the $J'(\omega)$ (Fig. 4) and $J''(\omega)$ (Fig.5) of filled PS compared to the unfilled PS. As an example in Fig. 4 at ω equals to 100 radian/s the value of J' changed from $8.7 \cdot 10^{-6}$ to $4 \cdot 10^{-6} \text{ Pa}^{-1}$ by the addition of 7% RSS. This is caused by the formation of the network (physical network-like structure), hence the increase in the strength of the PS/RSS composite.

Tan δ is plotted in Fig. 6 as a function of frequency for filled and unfilled PS. Tan δ measures the imperfection in the elasticity and it indicates the relative degree of viscous to elastic dissipation of the material. Therefore, tan δ is called the loss factor. Figure 6 shows a decrease in tan δ with the frequency followed by increasing again and the minimum of tan δ is in the range of about 25 to 80 radian/s for both of filled and unfilled PS. The minimum in tan δ reflects the minimum in loss energy per cycle of the sinusoidal deformation, which is related to the rubbery regime where the perfection of the elasticity due to the entanglements of the polymer chains. Tan δ is shown to increase by the addition of the fillers as seen in Fig. 6.

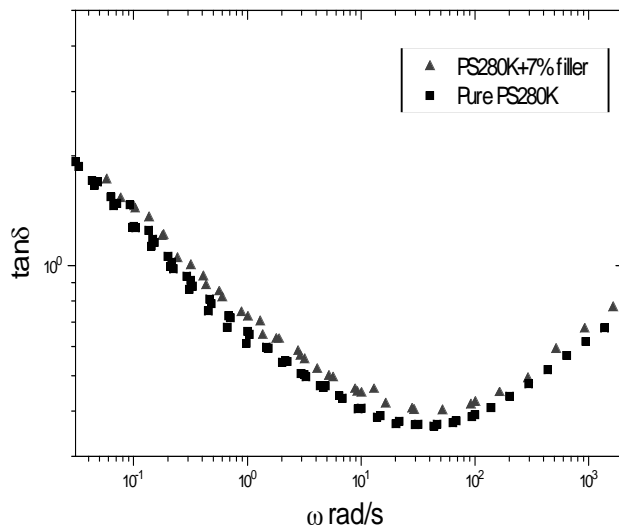


Figure 6. Master curve of tan δ for filled and unfilled PS280K vs ω at $T_0 = 160^\circ\text{C}$

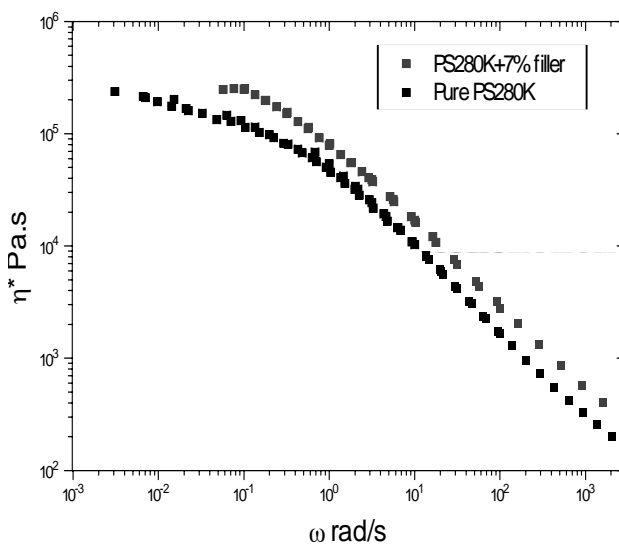


Figure 7. Master curve of η^* for filled and unfilled PS280K vs ω at $T_0 = 160^\circ\text{C}$

The complex viscosity η^* is plotted versus ω in Fig. 7 and it is related to the dynamic viscosity, η' as, $\eta^* = \eta' - i\eta''$. η^* decreases monotonically with increasing ω and falls by many orders of magnitude as shown in Fig. 7. At very low frequencies, particularly in the case of unfilled PS, η^* approaches the zero-shear viscosity, ζ_0 (Newtonian viscosity branch) where the viscosity is independent on the frequency and ζ_0 can be obtained

from G'' and ω as, $\eta_0 = \lim_{\omega \rightarrow 0} \frac{G''(\omega)}{\omega}$ (Mahmoud Halim

Abdel-Goad, A., 2000). Figure 7 shows an increase in the viscosity for 7% fiber-filled PS compared to unfilled PS, particularly in the Newtonian viscosity branch. Since the values of η_0 are about 2.8×10^5 and 1.1×10^5 Pa.s for PS composite and neat PS, respectively. This increase in η^* by the incorporation of 7% RSS may be because the formation of a layer of immobilized polymer chains around the fiber. That is generally as described by Einstein equation, which predicts the viscosity of a Newtonian fluid containing a very dilute suspension of rigid spheres as, $\eta = \eta_l (1 + K_E \times \phi)$ where η is the viscosity of the mixture, η_l is the viscosity of the suspending liquid and ϕ is the volume fraction of fillers and K_E is the Einstein coefficient which for spherical particles is 2.5 and vary according to the particle shape and orientation (Hornsby, P.R., 1999) shows in Fig. 7, the presence of fibers in viscous PS melts not only increases its viscosity but also influences its shear rate dependency which alters the beginning of frequencies-independent. Where the beginning of frequencies-independent is shifted by the incorporation of 7% RSS filler from 0.032 (in the case for neat PS) to 0.057 radian/s (in the case of PS composite) as shown in Fig. 7.

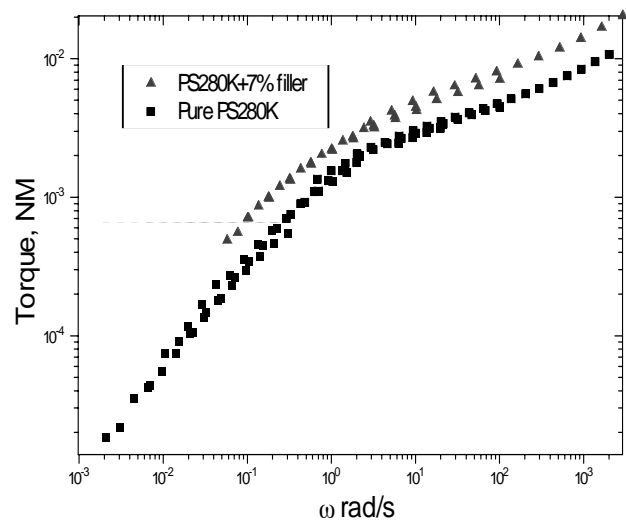


Figure 8. Master curve of the torque for filled and unfilled PS280K vs ω at $T_0 = 160^\circ\text{C}$

The torque is investigated for the samples of neat PS and PS composite and logarithmically plotted as a function of the frequency as shown in Fig. 8. In this Figure the torque increases monotonically by many orders of magnitude with increasing up to about 4 radian/s then increases gradually. And the value of the torque for PS composite is higher than this of neat PS. As shown in Fig. 8, at 100 radian/s the torque increased from $4.7 \cdot 10^{-3}$ to $7 \cdot 10^{-3}$ NM. This because of the increase in the strength and stiffness of the PS by the addition of the RSS since the formation of a polymer matrix-fibers network consisted of polymer chains and fibers.

The shear relaxation modulus $G(t)$ for fiber-filled and unfilled PS is plotted against time with logarithmic scales in Fig. 9. The modulus $G(t)$ defined as the relaxation stress/strain ratio at constant deformation. At intermediate times $G(t)$ flattens somewhat at a level which is associated with the average spacing between entanglement coupling points. The height of $G(t)$ at the intermediate time (rubbery zone) is the plateau modulus, G_N^0 . In this study G_N^0 was evaluated from the rubbery zone in $G(t)$ to be about 0.23 and 0.18 MPa for 7% fiber filled-PS and unfilled PS, respectively as shown in Fig. 9. And generally Fig. 9 shows higher $G(t)$ for fiber-filled samples than this in the cases of unfilled sample. This again evidence for the high stiffness and strength of composites compared to neat PS. The width of the rubber-like regime for PS composite is observed to be longer than this of neat PS. It may be because of the formation of the temporary entanglements between the cellulosic fiber and the polymer chains and that is proved too at the longest relaxation time. At long times $G(t)$ falls sharply and approaches the longest relaxation time, τ_d . τ_d is defined as the time required to leave the chain completely its tube (the constraint of their surrounding chains) by reptation or snake-like motion. τ_d is enlarged for fiber-filled PS, since it increases from around 1.1 second to 4 seconds by the addition of 7% filler as shown in Fig. 9. That is due to the resistance of the fiber for the mobility of the chain due to the formation of the temporary entanglements. Therefore, the time needed for the chains to move within the constraint of their surrounding molecules is long.

The observations in Fig. 9 are found for the shear creep stress, $J(t)$ in Fig. 10, as the logarithmic plots of $J(t)$ have roughly the appearance of mirror image of $G(t)$ plot reflected in the time axis. In Fig. 10 $J(t)$ for neat PS and 7% fiber-filled PS are plotted as a function of time. This Figure indicates that $J(t)$ increases with time and the effect of the RSS addition is clear since values of $J(t)$ at 0.1 second are 1.14×10^{-5} and 7.94×10^{-6} Pa⁻¹ for filled and unfilled PS, respectively, as explained above due to the networks formation.

The relaxation spectrum H (Fig. 11) and retardation spectrum L (Fig. 12) are logarithmically plotted versus time. They refer to the deformation in shear. Besides, they are useful qualitatively in gauging the distribution of relaxation and retardation mechanisms, respectively in different regions of the time scale. In polymers a broad spectrum of relaxation times exists due to the large freedom of polymer chain configurations. These

Figures indicate the effect of the addition of fiber to the PS, since the increase in the strength and stiffness of PS by the addition of RSS reflects in relaxation and retardation spectrum as shown in Fig. 11 and 12. Since at 0.01 second $H(t)$ increases from about 1.6×10^4 to 3.7×10^4 Pa and $L(t)$ changes from 1×10^{-6} to 2×10^{-6} Pa⁻¹ by the incorporation of 7% filler to the sufficiently high molecular weight PS.

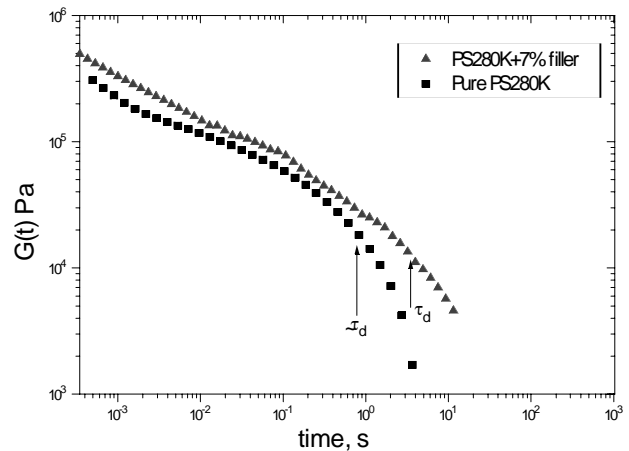


Figure 9. Master curve of $G(t)$ for filled and unfilled PS280K vs time at $T_o = 160^\circ\text{C}$

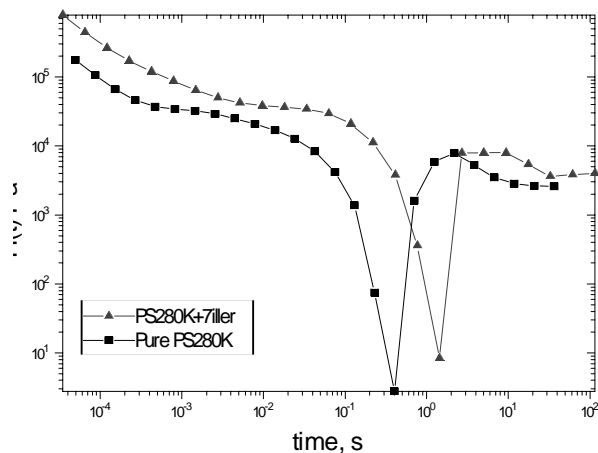


Figure 10. Master curve of $J(t)$ for filled and unfilled PS280K vs time at $T_o = 160^\circ\text{C}$

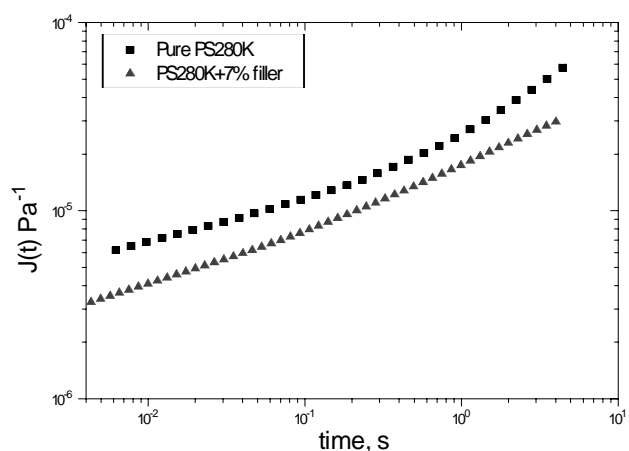


Figure 11. Master curve of $H(t)$ for filled and unfilled PS280K vs time at $T_o = 160^\circ\text{C}$

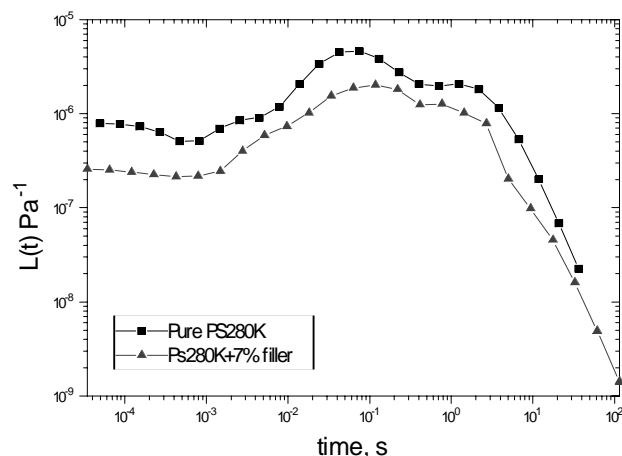


Figure 11. Master curve of $H(t)$ for filled and unfilled PS280K vs time at $T_o = 160^\circ\text{C}$

4. Conclusions

The viscoelastic properties are improved by the addition of residual softwood sawdust (RSS) and their values rise with filler loading. Therefore, fiber-filled composites have much potential for applications of environmental friendly plastics owing to their strength and stiffness.

Acknowledgments

The financial support by the International Bureau in Germany, helpful discussions of Dr. W. Pyckhout-Hintzen (IFF,FZJ, Research center Juelich, Germany) are greatly acknowledged.

References

- Angles, M.N., Salvado, J. and Dufresne, A., 1999, "J. of Applied Polymer Science," Vol. 74, pp. 1962-1977.
- Bledzki, A.K., Reihmane, S. and Gassan, J., 1996, "J. of Applied Polymer Science," Vol. 59, pp. 1329-1336.
- Fang, Z. and Hu, Q., 1999, "Die Angewandte Makromolekulare Chemie," Vol. 265(Nr.4474), pp. 1-4.
- Felix, J.M. and Gatenholm, P., 1991, "J. of Applied Polymer Science," Vol. 42, pp. 609-620.
- Ferry, J.D., 1980, "Viscoelastic Properties of Polymers", 3rd ed. Wiley, New York.
- Gatenholm, P., Bertilsson, H. and Mathiasson, A., 1993, "J. of Applied Polymer Science," Vol. 49, pp. 197-208.
- George, J., Bhagawan, S.S., Prabhakaran, N. and Thomas, S., 1995, "J. of Applied Polymer Science," Vol. 57, pp. 843-854.
- Heinrich, G. and Klüppel, M., 2002, "Advances in Polymer Science," Vol. 160, pp. 1-29.
- Hornsby, P.R., 1999, "Advances in Polymer Science," Vol. 139, pp. 1-213.
- Hu, X., et al. 2003, "Macromolecules," Vol. 36, pp. 823-829.
- Kim, J.I., Ryu, S.H. and Y.W.Chang., 2000. "J.of Applied Polymer Science," Vol. 77, pp. 2595-2602.
- Lee, K.M. and Han, C.D., 2003, "Polymer," Vp.: 44, pp. 4573-4588.
- Lowys, M.P., Desbrieres, J. and Rinaudo, M., 2000, "Food Hydrocolloids," Vol. 15, pp. 25-32.
- Mahmoud A.-Halim Abdel-Goad, 2000, PhD thesis, Muenster University, Germany.
- Marchant, D. and Jayaraman, K., 2002, Ind.Eng.Chem.Res., Vol. 41, pp. 6402-6408.
- Mcginness, G.B. and Bradaigh, C.M.O., 1997, "J.Non-Newtonian Fluid Mech," Vol. 73, pp. 1-28.
- Mitsubishi, K., 1997, "Die Angewandte Makromolekulare Chemie," Vol. 248, pp. 73-83.
- Mohanty, A.K., Misra, M. and Hinrichsen, H., 2000, "Macromol.Mater.Eng," Vol. 276/277, pp. 1-24.
- Nam, J.D. and Sefferis, J.C., 1999, "J.of Polymer Science:Part B:Polymer Physics," Vol. 37, pp. 907-918.
- Pearson, D., Fetters, L. and Grassley, W., 1994, "Macromolecules," Vol. 27, pp. 711-719.
- Ray, S.S., Maiti, P., Okamoto, M., Yamada, K. and Ueda, K., 2002, "Macromolecules," Vol. 35, pp. 3104-3110.
- Roy, D., Bhowmick, A.K. and De, S.K., 1993, "J. of Applied Polymer Science," Vol.49, pp. 263-273.
- Saha, A.K., Das, S., Bhatta, D. and Mitra, B.C., 1999, "J. of Applied Polymer Science," Vol. 71, pp. 1505-1513.
- Solomon, M.J., et al. 2001, "Maromolecules," Vol. 34, pp. 1864-1872.
- Swerin, C., 1998, "Colloids and Surfaces A: Physicochemical and Engineering Aspects," Vol. 133, pp. 279-294.
- Tavman, J.H., 1996, "J.of Applied Polymer Science," Vol. 62, pp. 2161-2167.
- Wang, X., Wu, O., Dong, J., Hu, Y. and Qi, Z., 2002, "J.of Applied Polymer Science," Vol. 85, pp. .2913-2921.
- Zhang. Q. and Archer, L.A., 2002, "Langmuir," Vol. 18, pp. 10435-10442.